

Towards Reliable Negative Sampling for Recommendation with Implicit Feedback via In-Community Popularity

Chen Chen

uicetomeetn@gmail.com
College of Computer Science and
Technology, Jilin University
Changchun, Jilin, China

Haobo Lin

would1920@gmail.com
College of Computer Science and
Technology, Jilin University
Changchun, Jilin, China

Yuanbo Xu*

Yuanbox@mails.jlu.edu.cn
College of Computer Science and
Technology, Jilin University
Changchun, Jilin, China

Abstract

Learning from implicit feedback is a fundamental problem in modern recommender systems, where only positive interactions are observed and explicit negative signals are unavailable. In such settings, negative sampling plays a critical role in model training by constructing negative items that enable effective preference learning and ranking optimization. However, designing reliable negative sampling strategies remains challenging, as they must simultaneously ensure realism, hardness, and interpretability. To this end, we propose **ICPNS (In-Community Popularity Negative Sampling)**, a novel framework that leverages user community structure to identify reliable and informative negative samples. Our approach is grounded in the insight that item exposure is driven by latent user communities. By identifying these communities and utilizing in-community popularity, ICPNS effectively approximates the probability of item exposure. Consequently, items that are popular within a user's community but remain unclicked are identified as more reliable true negatives. Extensive experiments on four benchmark datasets demonstrate that ICPNS yields consistent improvements on graph-based recommenders and competitive performance on MF-based models, outperforming representative negative sampling strategies under a unified evaluation protocol.

CCS Concepts

• Information System → Recommender System.

Keywords

Data Mining, Recommender System, Negative Sampling

1 Introduction

Implicit feedback such as clicks serves as the foundation for modern Recommender Systems (RS). Unlike explicit feedback such as ratings, implicit feedback suffers from the one-class problem: only positive interactions are observed, while negative signals are absent. Consequently, **negative sampling** selects unobserved items to represent user disinterest, which is critical for model training (see Figure 1 A). A fundamental challenge in negative sampling lies in the inherent ambiguity of unobserved interactions: an item may be unobserved either because the user genuinely dislikes it or because the user was never exposed to it (see Figure 1 B). This ambiguity introduces challenges in practice. First, aggressively sampling negatives risks selecting false negatives, exacerbating the False Negative Problem (FNP)[3, 23, 30]. Second, overly conservative sampling may lead to trivial negatives that slow down optimization. Moreover,

*Corresponding Author.

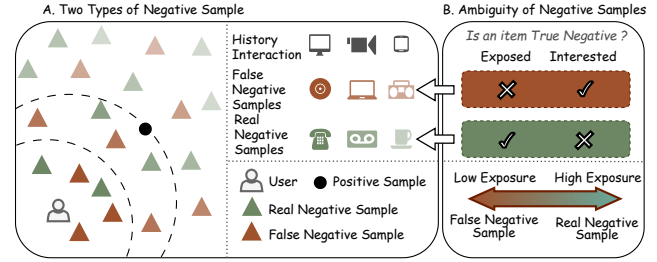


Figure 1: Overview of negative sampling ambiguity and the motivation of ICPNS. (A) Two types of unobserved items under implicit feedback. Triangles with darker colors indicate higher sample hardness; as hardness increases, the likelihood of false negatives also increases. (B) The inherent ambiguity of negative samples: true negatives arising from genuine disinterest and false negatives caused by lack of exposure. ICPNS approximates item exposure using in-community popularity, treating unclicked but community-popular items as more reliable negatives.

when negative samples are selected based on opaque heuristics or model scores alone, it becomes difficult to interpret why a specific item is regarded as a negative instance. Taken together, these challenges suggest that a *reliable* negative sampling strategy should satisfy several essential requirements. Specifically, it should prioritize samples that are likely to reflect genuine disinterest rather than missing exposure (*realness*), provide sufficiently informative training signals (*hardness*), and offer a transparent rationale for negative selection (*interpretability*).

Existing negative sampling strategies struggle to satisfy these criteria simultaneously (see Table 1). The most basic approach, **Random Negative Sampling (RNS)**[7, 8, 22, 28], randomly selects non-interacted items as negatives. While unbiased and simple to implement, RNS fails all the three criterion due to its randomness. As an improvement, **Popularity Negative Sampling (PNS)**[4, 9, 15, 21] assumes that globally popular items are more likely to have been exposed to users. If a user has not interacted with a globally popular item, it is likely a true negative. However, PNS relies on a "global exposure" assumption, ignoring that exposure is highly personalized and community-dependent. It fails to capture the nuance that users are typically exposed to items within their specific interest groups, leading to suboptimal interpretability. **Hard negative sampling (HNS)**[17, 24, 29, 31] sample items that the system confuses with positives (e.g., items with higher prediction scores), potentially accelerating convergence since it provide

Table 1: Comparison of representative negative sampling strategies with respect to realness, hardness, and interpretability.

Strategy	Realness	Hardness	Interpretability
RNS	✗	✗	✗
PNS	✗	✗	✓
HNS	✗	✓	✗
ICPNS	✓	✓	✓

stronger negative signals. However, high-scoring unobserved items are often valid recommendations that the user has not yet seen[30]. Treating them as negatives introduces severe noise, violating realness and degrading (see Figure 1 D). Some non-sampling work also inspired this work. EXMF[16] and FAWMF[2] explicitly model the item exposure, which records the recommended but not interacted items, provides realness of negative samples.

To bridge these gaps, we revisit a fundamental premise of negative sampling: a non-interaction reflects genuine disinterest only if the user has been exposed to the item. Without exposure, a missing interaction is merely unobserved. From this perspective, identifying reliable negative samples reduces to estimating the probability of item exposure. Motivated by a sociological insight that exposure is structured by user communities[19, 33], we propose **In-Community Popularity Negative Sampling (ICPNS)**. ICPNS models exposure at the community level rather than globally: if an item is popular within a user’s latent community, it is likely to have been exposed to that user. Consequently, an unobserved interaction with a community-popular item constitutes a strong signal of disinterest. Based on this principle, ICPNS samples negatives from items that are popular within a user’s community but individually unobserved, using a lightweight two-stage pipeline that remains computationally efficient.

The main contributions of this work are summarized as follows:

- **A Community-Based View of Exposure.** We reinterpret negative sampling through exposure modeling and argue that exposure is inherently community-structured rather than globally uniform.
- **The ICPNS Framework.** We propose In-Community Popularity Negative Sampling, a simple yet effective framework that leverages latent user communities to sample reliable and informative negatives, directly addressing the realness, hardness, and interpretability criteria.
- **Empirical Validation.** Extensive experiments on four benchmark datasets demonstrate improvements over representative negative sampling strategies.

2 Preliminary

2.1 Notations

Let $\mathcal{U} = \{u_1, u_2, \dots, u_N\}$ and $\mathcal{I} = \{i_1, i_2, \dots, i_M\}$ denote the sets of N users and M items, respectively. The user-item interactions are represented by a binary matrix $\mathbf{X} \in \{0, 1\}^{N \times M}$, where an entry $x_{ui} = 1$ indicates an observed interaction (e.g., click, purchase) between user $u \in \mathcal{U}$ and item $i \in \mathcal{I}$, while $x_{ui} = 0$ denotes an unobserved interaction. Note that unobserved interactions are inherently

ambiguous, representing either a genuine lack of interest (true negative) or a lack of exposure (potential positive). For each user u , we denote the set of interacted items as $\mathcal{I}_u^+ = \{i \in \mathcal{I} \mid x_{ui} = 1\}$.

2.2 Problem Formulation

The primary objective of recommendation with implicit feedback is to predict a user’s preference for items they have not yet interacted with. Formally, the task is to learn a prediction function $f: \mathcal{U} \times \mathcal{I} \rightarrow \mathbb{R}$ parameterized by Θ , which estimates a preference score \hat{x}_{ui} for a user-item pair (u, i) :

$$\hat{x}_{ui} = f(u, i \mid \Theta). \quad (1)$$

For each user u , RS aims to generate a personalized ranked list \mathcal{L}_u , containing items from the unobserved set $\mathcal{I} \setminus \mathcal{I}_u^+$, sorted in descending order of their predicted scores.

2.3 Negative Sampling

During training, a widely adopted objective is the Bayesian Personalized Ranking (BPR) loss[22], which optimizes the pairwise ranking between observed (positive) and unobserved (negative) items. The loss function is defined as:

$$\mathcal{L}_{\text{BPR}} = \sum_{(u, i, i^-) \in \mathcal{D}_s} -\ln \sigma(\hat{x}_{ui} - \hat{x}_{ui^-}) + \lambda \|\Theta\|_2^2, \quad (2)$$

where $\mathcal{D}_s = \{(u, i, i^-) \mid u \in \mathcal{U}, i \in \mathcal{I}_u^+, i^- \in \mathcal{I} \setminus \mathcal{I}_u^+\}$ represents the set of training triplets. Here, $\sigma(\cdot)$ is the sigmoid function, and λ controls the L_2 regularization strength. Negative sampling is the process of selecting a negative item i^- for a given user u and positive item i . It can be formally viewed as sampling from a negative distribution P_{neg} :

$$i^- \sim P_{\text{neg}}(\cdot \mid u, i). \quad (3)$$

The sampled item i^- is then used for optimization.

3 Methodology

3.1 Encoder

ICPNS is a backbone-agnostic negative sampling framework. The role of the encoder is to learn user/item embeddings for (1) constructing a meaningful user embedding space for community identification, and (2) providing preference scores for BPR optimization. Therefore, ICPNS can be instantiated with various backbone such as MF-based and graph-based encoder.

3.1.1 MF-based Encoder. Matrix Factorization (MF) models user preferences by assuming that the interaction matrix $\mathbf{X} \in \mathbb{R}^{N \times M}$ admits a low-rank approximation. Specifically, MF seeks to decompose \mathbf{X} into the product of two low-dimensional embedding matrices:

$$\mathbf{X} \approx \mathbf{E}_U \mathbf{E}_I^T, \quad (4)$$

where $\mathbf{E}_U \in \mathbb{R}^{N \times D}$ and $\mathbf{E}_I \in \mathbb{R}^{M \times D}$ denote the user and item embedding matrices, respectively, and $D \ll \min(N, M)$ is the embedding dimension.

The predicted preference score between user u and item i is given by the inner product of their corresponding latent embedding:

$$\hat{x}_{ui} = \mathbf{e}_u^T \mathbf{e}_i, \quad (5)$$

where \mathbf{e}_u and \mathbf{e}_i are the u -th and i -th rows of \mathbf{E}_U and \mathbf{E}_I .

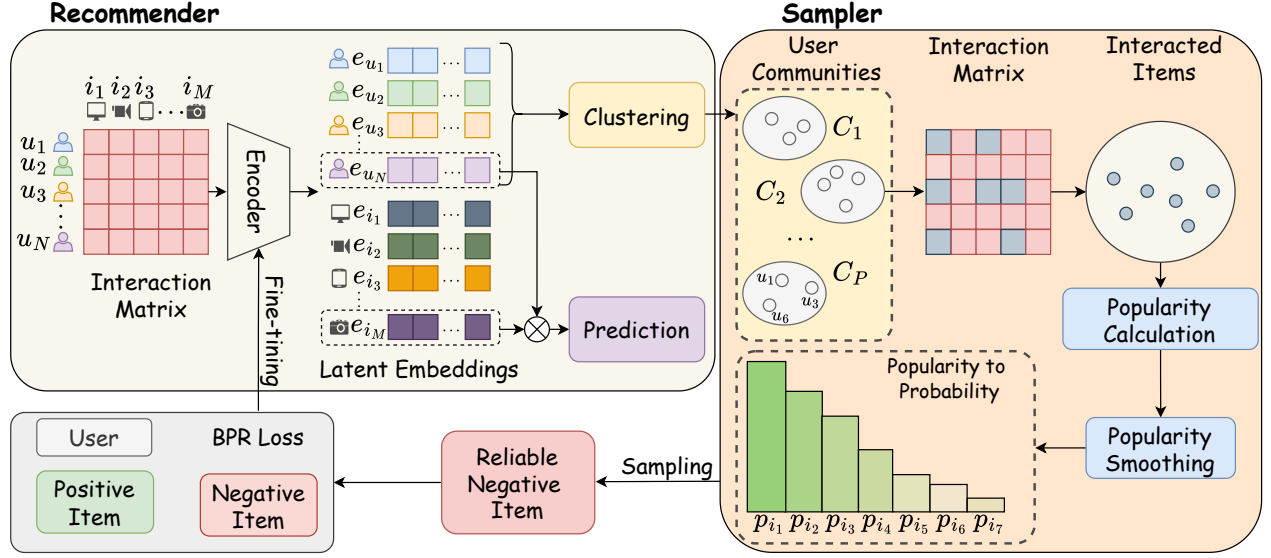


Figure 2: The detailed framework of ICPNS. After encoder is well-pretrained by RNS, the model switches to our ICPNS strategy. Here, users are clustered into latent communities based on pre-trained embeddings, and in-community popularity is leveraged to sample reliable negative items.

3.1.2 Graph-based Encoder. Graph-based encoders learn latent user and item embeddings by performing message passing over the bipartite interaction graph, explicitly modeling high-order collaborative signals beyond direct interactions. Let D denote the embedding dimension. We initialize the embeddings of all users and items in a matrix $E^{(0)} \in \mathbb{R}^{(N+M) \times D}$.

The user–item interaction graph is commonly represented by a bipartite adjacency matrix:

$$A = \begin{pmatrix} \mathbf{0} & X \\ X^T & \mathbf{0} \end{pmatrix} \in \mathbb{R}^{(N+M) \times (N+M)}, \quad (6)$$

where X denotes the interaction matrix. To stabilize message propagation, the adjacency matrix is typically symmetrically normalized as $\tilde{A} = D^{-1/2} A D^{-1/2}$, where D is the diagonal degree matrix with $D_{ii} = \sum_j A_{ij}$.

Graph-based encoders update node embeddings by aggregating embeddings from neighboring nodes according to the graph structure. Without loss of generality, we illustrate this process using LightGCN as an example. LightGCN employs a simplified, parameter-free propagation rule given by:

$$E^{(k+1)} = \tilde{A} E^{(k)}. \quad (7)$$

After K propagation layers, embeddings from different layers capture collaborative signals at varying neighborhood ranges. A common practice in graph-based recommenders is to aggregate multi-layer embeddings via a weighted sum:

$$E^* = \sum_{k=0}^K \alpha_k E^{(k)}, \quad (8)$$

where α_k are hyperparameters controlling the contribution of each layer, typically set to $1/(K+1)$. The final embedding matrix E^* is then split into user embeddings $E_{u_j}^* \in \mathbb{R}^{N \times D}$ and item embeddings

$E_{i_j}^* \in \mathbb{R}^{M \times D}$, with e_u and e_i denoting the embeddings of user u and item i , respectively.

3.2 ICPNS Negative Sampler

The proposed ICPNS comprises three key steps: (1) identifying latent user communities, (2) computing item popularity within each community to capture localized exposure patterns, and (3) sampling negative items according to a smoothed in-community popularity distribution.

3.2.1 Community Identification. We hypothesize that users located close to each other in the learned embedding space tend to share similar exposure patterns or latent interests. To capture such structure, we apply clustering algorithms to partition the user set \mathcal{U} into P disjoint communities $C = \{C_1, C_2, \dots, C_P\}$, satisfying:

$$\bigcup_{p=1}^P C_p = \mathcal{U}, \quad C_p \cap C_{p'} = \emptyset \quad \forall p \neq p'. \quad (9)$$

The community assignments are fixed after the pre-training stage and remain unchanged during fine-tuning.

3.2.2 In-community Popularity Computation. For each identified community C_p , we compute an in-community interaction count vector $v_p \in \mathbb{R}^M$, where each entry corresponds to the interaction frequency of an item within the community:

$$(v_p)_j = \sum_{u \in C_p} \mathbb{1}(x_{uj} = 1), \quad \forall j \in \mathcal{I}. \quad (10)$$

To mitigate bias toward globally popular items, we further derive a smoothed in-community popularity score. Specifically, for each community C_p , we define a popularity vector $s_p \in \mathbb{R}^M$ as:

$$(s_p)_j = ((v_p)_j)^\alpha, \quad (11)$$

Table 2: Statistics of four preprocessed datasets.

Dataset	Users	Items	Interactions	Sparsity
ML-100K	940	1017	80,393	91.59%
ML-1M	6,034	3,124	834,449	95.57%
Yelp	26,420	19,921	1,285,021	99.76%
Beauty	1,238	720	25,736	97.11%

where $\alpha \in [0, 1]$ is a smoothing hyperparameter. When $\alpha < 1$, the influence of items with extremely high interaction counts is suppressed, allowing less frequent but community-relevant items to contribute more effectively to negative sampling.

3.2.3 Negative Sampling Procedure. During the fine-tuning stage, ICPNS is employed to sample negative items. For each positive training pair (u, i) with $u \in C_p$, a negative item i^- is sampled from the set of unobserved items $\mathcal{I} \setminus \mathcal{I}_u^+$. The probability of selecting an item j as a negative sample is defined according to its in-community popularity, normalized over the candidate set:

$$P(i^- = j | u \in C_p) = \frac{(s_p)_j}{\sum_{k \in \mathcal{I} \setminus \mathcal{I}_u^+} (s_p)_k}, \quad j \in \mathcal{I} \setminus \mathcal{I}_u^+. \quad (12)$$

3.3 Two-Stage Training Pipeline

Our model is trained in a two-stage pipeline to maximize the effectiveness of the encoder and the negative sampler.

Stage 1: Pre-training. We first pre-train the encoder to learn a stable and informative embedding space. In this stage, the model is optimized using the BPR loss with RNS, which serves as a standard and robust initialization strategy for collaborative filtering models.

Stage 2: Fine-tuning with ICPNS. After pre-training, we fix the community assignments inferred from the pretrained encoder and perform clustering only once considering stability. The model is then fine-tuned by replacing RNS with the proposed ICPNS, while continuing to optimize the BPR loss with negative samples drawn from the in-community popularity distribution.

A detailed algorithmic description of the two-stage training pipeline is provided in AppendixA.

3.4 Complexity Analysis

We focus on the computational efficiency of negative sampling and exclude the overhead of encoder propagation and clustering during initialization. As shown in Figure 1 D, all compared methods achieve $O(1)$ time complexity per sampled negative item.

In practice, HNS may incur a larger constant factor due to the need to evaluate preference scores over multiple candidate items. For ICPNS, constant-time sampling is achieved via the Alias Method, which enables $O(1)$ sampling from a discrete non-uniform distribution after preprocessing. Specifically, for each community-level popularity distribution, an alias table is constructed with $O(|\mathcal{I}_c|)$ preprocessing time, where \mathcal{I}_c denotes the item set of community c .

4 Experiment

In this section, we conduct extensive experiments to systematically evaluate the effectiveness of ICPNS. Specifically, our experimental study is designed to address the following key research questions:

- **Q1:** Can ICPNS consistently improve recommendation performance across diverse datasets and backbone models?
- **Q2:** How does ICPNS compare with existing negative sampling strategies in terms of both effectiveness and computational efficiency?
- **Q3:** Does ICPNS generate negative samples that are both real and hard?
- **Q4:** To what extent are the individual components of ICPNS essential to its overall performance?
- **Q5:** How does different clustering algorithms affect the performance of ICPNS?
- **Q6:** How do key hyperparameters influence the performance of ICPNS?

4.1 Experimental Settings

4.1.1 Datasets. We evaluate the proposed ICPNS on four publicly accessible benchmark datasets, covering diverse domains including movies, e-commerce, local businesses and varying data sparsity levels.

- **ML-100K & ML-1M¹:** Widely used movie recommendation datasets collected by GroupLens Research, containing user ratings on movies.
- **Amazon-Beauty²:** A subset of the Amazon product review dataset, representing a sparse e-commerce scenario.
- **Yelp³:** A dataset adopted from the 2018 Yelp Challenge, recording user check-ins at local businesses like restaurants and bars.

Preprocessing: Since all four datasets are rating-based, to fit it into implicit feedback task, we first binarized the ratings by excluding interactions below half of the highest rating. We filter out cold-start users and items with less than k interactions ($k = 10$ for ML-100K, ML-1M and Beauty, $k = 20$ for Yelp). The detailed statistics of the processed datasets are summarized in Table 2.

4.1.2 Baseline Strategies. We compare ICPNS against the following negative sampling strategies:

- **RNS [22]:** Uniformly samples unobserved items as negative instances.
- **PNS [21]:** Samples negative items according to their global popularity distribution. Following prior work, we apply popularity smoothing with a smoothing factor of $\alpha = 0.1$ to mitigate the dominance of extremely popular items.
- **HNS [31]:** Selects hard negatives based on model-predicted preference scores. Following prior work, for each user, we first sample $s = 10$ candidate items and then choose the item with the highest predicted score assigned by current model as the negative sample.

4.1.3 Backbone. To demonstrate the potential of ICPNS on different backbone models, we select models from two mainstream general recommendation categories as follows:

- **Matrix Factorization (MF-based):** BPR[22] (UAI '09), DMF[27] (IJCAL '17), NeuMF[8] (WWW '17).

¹<https://grouplens.org/datasets/movielens>

²<https://jmcauley.ucsd.edu/data/amazon/>

³<https://www.kaggle.com/datasets/yelp-dataset/yelp-dataset/versions/1>

Table 3: Performance comparison of various negative sampling strategies across different backbone models. Boldface indicate the best results for each model.

Model	Strategy	ML-100K				ML-1M				Yelp				Beauty			
		Rec	MRR	NDCG	Pre												
BPR	RNS	0.266	0.418	0.264	0.170	0.172	0.416	0.238	0.179	0.070	0.093	0.056	0.030	0.231	0.145	0.146	0.043
	PNS	0.253	0.408	0.254	0.162	0.174	0.416	0.237	0.177	0.070	0.094	0.056	0.029	0.231	0.145	0.144	0.043
	HNS	0.258	0.398	0.250	0.159	0.176	0.418	0.239	0.178	0.085	0.115	0.069	0.036	0.234	0.159	0.155	0.043
	ICPNS	0.269	0.413	0.257	0.162	0.176	0.415	0.238	0.178	0.082	0.113	0.068	0.035	0.224	0.147	0.147	0.041
NeuMF	RNS	0.253	0.415	0.259	0.162	0.161	0.380	0.217	0.166	0.063	0.079	0.049	0.025	0.232	0.150	0.149	0.043
	PNS	0.256	0.421	0.260	0.162	0.160	0.377	0.214	0.164	0.059	0.075	0.046	0.024	0.231	0.150	0.149	0.043
	HNS	0.254	0.419	0.251	0.157	0.183	0.434	0.245	0.179	0.069	0.093	0.056	0.029	0.229	0.154	0.151	0.044
	ICPNS	0.263	0.424	0.267	0.167	0.188	0.443	0.254	0.186	0.064	0.079	0.049	0.025	0.234	0.144	0.147	0.043
DMF	RNS	0.259	0.414	0.256	0.161	0.160	0.399	0.223	0.166	0.061	0.092	0.051	0.027	0.232	0.147	0.146	0.044
	PNS	0.256	0.405	0.250	0.158	0.164	0.395	0.224	0.168	0.060	0.089	0.049	0.025	0.198	0.127	0.125	0.036
	HNS	0.248	0.400	0.246	0.154	0.160	0.394	0.218	0.163	0.069	0.094	0.061	0.037	0.213	0.132	0.130	0.040
	ICPNS	0.265	0.398	0.254	0.158	0.165	0.408	0.228	0.169	0.065	0.093	0.054	0.031	0.231	0.143	0.142	0.043
NGCF	RNS	0.274	0.460	0.282	0.175	0.175	0.420	0.239	0.178	0.072	0.095	0.057	0.030	0.244	0.160	0.158	0.045
	PNS	0.272	0.452	0.280	0.177	0.176	0.412	0.236	0.177	0.070	0.095	0.056	0.029	0.240	0.146	0.149	0.045
	HNS	0.279	0.465	0.290	0.178	0.192	0.450	0.261	0.192	0.080	0.107	0.065	0.034	0.244	0.169	0.167	0.046
	ICPNS	0.323	0.551	0.356	0.219	0.208	0.504	0.304	0.225	0.086	0.123	0.073	0.037	0.262	0.222	0.201	0.050
LightGCN	RNS	0.276	0.450	0.281	0.175	0.183	0.429	0.249	0.186	0.075	0.104	0.062	0.032	0.234	0.150	0.147	0.043
	PNS	0.270	0.445	0.275	0.172	0.182	0.431	0.248	0.184	0.073	0.102	0.060	0.031	0.232	0.145	0.144	0.043
	HNS	0.284	0.476	0.288	0.179	0.206	0.478	0.279	0.202	0.084	0.118	0.071	0.035	0.249	0.153	0.154	0.046
	ICPNS	0.311	0.514	0.332	0.204	0.212	0.504	0.304	0.224	0.089	0.126	0.076	0.038	0.260	0.184	0.179	0.050
LightGCL	RNS	0.270	0.435	0.271	0.171	0.176	0.435	0.247	0.182	0.084	0.113	0.068	0.035	0.243	0.146	0.149	0.045
	PNS	0.257	0.426	0.261	0.164	0.181	0.441	0.252	0.185	0.086	0.117	0.070	0.035	0.248	0.155	0.154	0.045
	HNS	0.272	0.445	0.269	0.166	0.1995	0.460	0.266	0.197	0.087	0.118	0.072	0.035	0.253	0.149	0.152	0.046
	ICPNS	0.316	0.538	0.354	0.227	0.201	0.465	0.271	0.201	0.094	0.137	0.082	0.041	0.261	0.173	0.170	0.049

- **Graph-based:** NGCF[25] (SIGIR '19), LightGCN[7] (SIGIR '20), LightGCL[1] (ICLR '23).

4.1.4 Evaluation Protocol. For dataset partitioning, we employ a randomized splitting strategy, dividing interactions into training, validation, and testing sets with a ratio of 8:1:1, respectively. To evaluate the recommendation performance, we employ four widely adopted metrics: Recall @K (Rec@K), Precision, Normalized Discounted Cumulative Gain @K (NDCG@k), and Mean Reciprocal Rank @K (MRR @K), with $K = 10$ by default. For detailed definition, please refer to Appendix C.1. Recall and Precision measure the retrieval coverage and accuracy, while NDCG and MRR evaluate the quality of the ranking order. We report the average results over all users in the test set.

4.1.5 Implementation Details. Our framework is implemented using PyTorch and the RecBole[32] library. We adopt a two-stage training pipeline. **Pre-training Stage:** We train the backbone model with RNS for a maximum of 1000 epochs without early stopping to ensure fully converged and stable user embeddings for clustering. **Fine-tuning Stage:** We switch the sampler to ICPNS and fine-tune the model. The maximum epochs are set to 1000, with an early stopping patience of 20 epochs based on NDCG@10 performance on the validation set. Hyperparameters: We optimize all models using the Adam optimizer with a learning rate of $1e - 3$ and a batch size of 4096. The embedding size is fixed at 64 for all models

for fairness. For ICPNS, the number of user communities P is set to 8 for ML-100K/Beauty and 32 for ML-1M/Yelp. The popularity smoothing factor α is set to 0.1. All experiments are conducted on a Linux server equipped with an Intel Xeon Platinum 8352V CPU and an NVIDIA RTX 4090 GPU (24GB).

4.2 Overall Performance (Q1)

In this section, we comprehensively evaluate the performance of ICPNS against three baseline negative sampling strategies across six backbone models and four datasets. The detailed performance comparison is presented in Table 3.

Overall, ICPNS demonstrates robust improvements over the standard RNS baseline across most settings, validating its effectiveness in mining reliable negatives. Notably, while ICPNS yields competitive results on MF-based models (occasionally underperforming compared to HNS), it consistently and significantly outperforms all baseline strategies on graph-based models. This disparity suggests that ICPNS benefits substantially from the structural knowledge encoded by graph neural networks. Since ICPNS relies on clustering learned user embeddings, the high-quality embeddings propagated through the graph structure facilitate more precise clustering, thereby maximizing the efficacy of ICPNS.

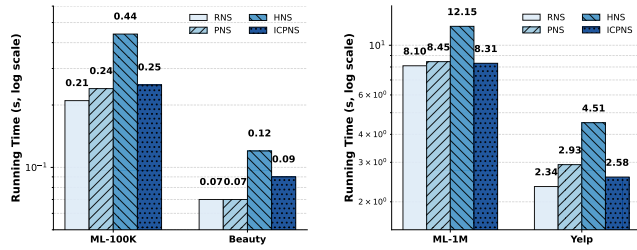


Figure 3: Comparison of training time per epoch across datasets. The y-axis is plotted on a logarithmic scale. To improve readability, small and large datasets are reported separately. ICPNS consistently achieves lower computational overhead compared to HNS.

4.3 Training Time Comparison (Q2)

To evaluate the practical utility of ICPNS, we compare its training efficiency against several representative negative sampling strategies. Figure 3 illustrates the average training time per epoch on a logarithmic scale. As analyzed in Section 3.4, all considered strategies, including RNS, PNS, HNS, and ICPNS theoretically achieve a sampling complexity of $O(1)$ per negative item. However, the experimental results reveal distinct gaps in actual execution time. Specifically, HNS consistently incurs the highest computational overhead across all datasets. This is attributed to its necessity to compute scores for multiple candidate items to identify hard negatives, which introduces a significantly larger constant factor in practice.

4.4 Realness and Hardness of Samples (Q3)

In this section, we analyze the realness and hardness of negative samples generated by ICPNS in comparison with baseline strategies.

Discussion. Realness: We introduce an auxiliary metric called **HoldoutHit@K** to approximate the risk of sampling false negatives. As this metric is not equivalent to exposure-based realness, we report its definition and experimental results in the Appendix B.1. **hardness:** As shown in Figure 4, ICPNS consistently generates harder samples compared to RNS and PNS. This superior hardness is an **inherent benefit of the community-based approach**: items that are popular within a user’s specific community usually share high semantic similarity with the user’s preferences. Consequently, the model assigns them higher prediction scores, making them naturally hard to discriminate.

4.5 Ablation Study (Q4)

To evaluate the effectiveness of each design choice in ICPNS, we perform ablation studies with three variants on the default ICPNS.⁴

We consider three ablation variants of ICPNS.

- **(Variant 1) w/o pretraining:** ICPNS without pretraining the encoder.
- **(Variant 2) w/o clustering:** ICPNS without clustering users into communities. We implement this by setting $P = 1$.

⁴Considering both simplicity and efficiency, we denote the default ICPNS by using LightGCN as encoder and k -means as clustering algorithm.

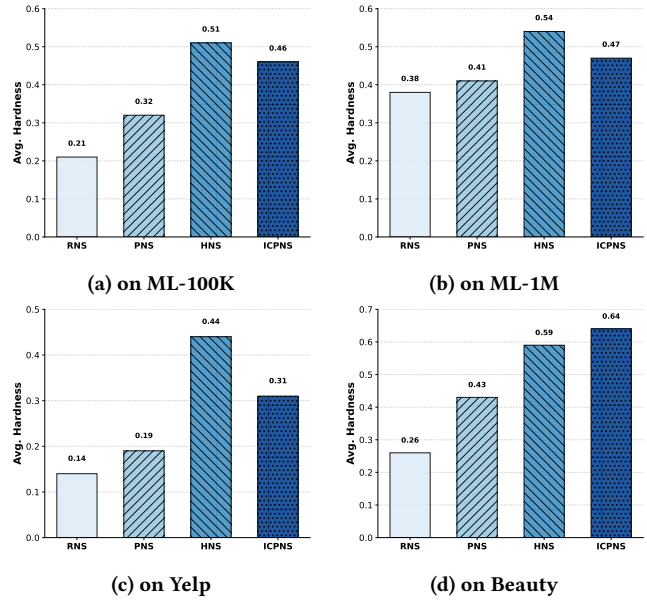


Figure 4: Comparison of hardness across different negative sampling strategies, averaged over all training epochs across four datasets.

- **(Variant 3) w/o smoothing:** ICPNS without popularity smoothing by setting $\alpha = 1$.

Discussion. The core of ICPNS is clustering users into different communities to leverage in-community popularity. Without pretraining, we cannot obtain high-quality user embeddings, and hence cannot cluster users into the appropriate communities. Without clustering, ICPNS actually degenerates to PNS, which is based on coarse-grained global popularity and fails to learn users’ fine-grained preferences. We also notice that ICPNS performs worse without smoothing. Given the inherent noise in implicit feedback, smoothing mitigates popularity bias and introduces necessary randomness. This allows the model to use popularity merely as a soft guidance signal, thereby facilitating the discovery of informative negatives.

4.6 Impact from the Quality of User Communities (Q5)

In this section, we detailedly evaluate how the clustering algorithms effects the performance of ICPNS. We evaluate the performance of ICPNS using LightGCN as the encoder on ML-100K and Beauty with different clustering algorithms. **Partition-based:** k -means. k -means partitions users into k disjoint clusters by minimizing the within-cluster variance. **Probability-based:** Gaussian Mixed Model (GMM). GMM models the user embedding distribution as a mixture of Gaussian components, allowing soft cluster assignments. **Density-based:** DBSCAN. DBSCAN identifies user communities as high-density regions in the embedding space and naturally treats sparse users as noise. **Hierarchical:** Agglomerative Clustering (AC). Agglomerative clustering builds a hierarchy of user communities by

Table 4: Ablation study evaluating the impact of key components, including pretraining, user clustering, and popularity smoothing, on recommendation performance across datasets. Default represents standard ICPNS.

Dataset	Variant	Rec	MRR	NDCG	Pre
ML-100K	Default	0.311	0.514	0.332	0.204
	w/o pretraining	0.157	0.298	0.161	0.102
	w/o clustering	0.270	0.445	0.275	0.172
	w/o smoothing	0.277	0.455	0.279	0.174
ML-1M	Default	0.212	0.504	0.304	0.224
	w/o pretraining	0.166	0.422	0.237	0.176
	w/o clustering	0.182	0.431	0.248	0.184
	w/o smoothing	0.183	0.513	0.287	0.202
Yelp	Default	0.089	0.126	0.076	0.038
	w/o pretraining	0.051	0.070	0.041	0.021
	w/o clustering	0.073	0.102	0.060	0.031
	w/o smoothing	0.079	0.113	0.065	0.033
Beauty	Default	0.260	0.184	0.179	0.050
	w/o pretraining	0.185	0.107	0.110	0.032
	w/o clustering	0.232	0.145	0.144	0.043
	w/o smoothing	0.251	0.176	0.171	0.048

Table 5: Performance comparison of ICPNS under different clustering algorithms, reflecting the impact of clustering quality.

Dataset	Clustering	Rec	MRR	NDCG	Pre
ML-100K	<i>k</i> -means	0.311	0.514	0.332	0.204
	GMM	0.335	0.560	0.374	0.240
	DBSCAN	0.330	0.555	0.371	0.239
	AC	0.347	0.603	0.404	0.251
	SC	0.350	0.596	0.401	0.247
Beauty	<i>k</i> -means	0.260	0.184	0.179	0.050
	GMM	0.266	0.226	0.206	0.051
	DBSCAN	0.294	0.257	0.231	0.059
	AC	0.277	0.270	0.234	0.056
	SC	0.280	0.225	0.209	0.054

iteratively merging the most similar clusters based on a linkage criterion. **Graph-based:** Spectral Clustering (SC). Spectral clustering operates on a similarity graph constructed from user embeddings and partitions users by leveraging the eigenstructure of the graph Laplacian.

Discussion. The performance comparison is shown in Table 5. Notably, with advanced clustering algorithm being adopted, the performance of ICPNS is accordingly upgrading. This indicates the learned community structure is vital in ICPNS since we need to calculate the in-community popularity.

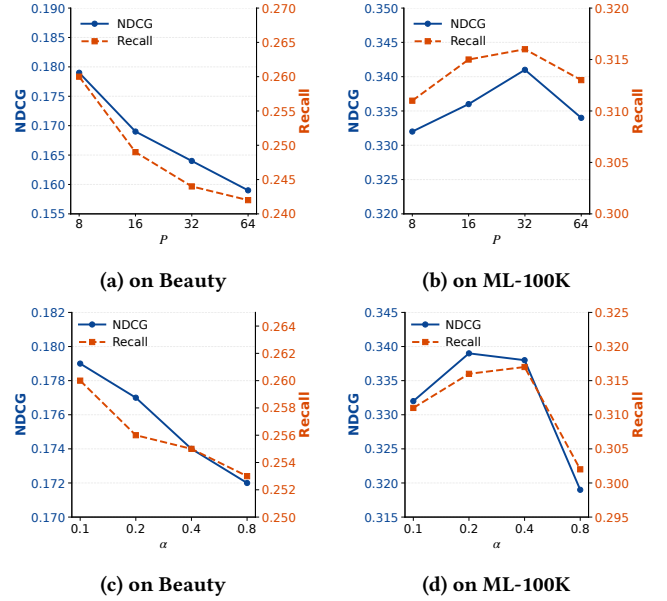


Figure 5: Parameter sensitivity analysis of ICPNS on Beauty and ML-100K. The top row (a–b) illustrates the impact of P , while the bottom row (c–d) displays the effect of α .

4.7 Hyperparameter Analysis (Q6)

In this section, we demonstrate the impact of two key hyperparameters in ICPNS on ML-100K and Beauty. Due to space constraint, result on Yelp and ML-1M is shown in Appendix B.2.

4.7.1 Impact of the Number of Communities P . We investigate the effect of the number of user communities by varying $P \in \{8, 16, 32, 64\}$ and. As shown in Figure 5 (a) and (b), the optimal community granularity is highly dataset-dependent. On the relatively small Beauty dataset, performance reaches its peak at $P = 8$ and consistently degrades as P increases, indicating that excessive partitioning leads to overly sparse communities and unstable signals for negative sampling. In contrast, for the larger ML-100K dataset, performance attains its maximum at $P = 32$, suggesting that finer-grained community structures are beneficial for capturing more nuanced user preference patterns when sufficient data are available.

4.7.2 Impact of the Popularity Smoothing Factor α . We further examine the sensitivity of the popularity smoothing factor α , which controls the degree of smoothing applied to in-community popularity. Figure 5 (c) and (d), reports NDCG and Recall under $\alpha \in \{0.1, 0.2, 0.4, 0.8\}$. Across both datasets, the model achieves its best performance with relatively small values of α from 0.1 to 0.4. As α increases to 0.8, performance consistently declines, indicating that excessive smoothing weakens informative popularity signals. These results highlight the necessity of moderate popularity smoothing for effectively mitigating popularity bias.

4.8 Case Study

To further demonstrate the effectiveness of ICPNS, we provide a case study on the ML-100K dataset with $P = 8$.

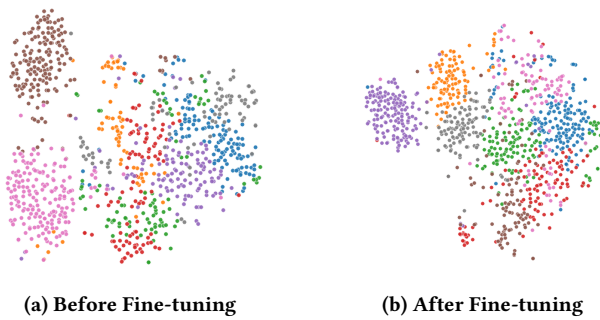


Figure 6: Visualization of community structure before and after fine-tuning with ICPNS at $P = 8$.

Table 6: Clustering quality metrics before and after fine-tuning on ML-100K. Lower Silhouette and Calinski–Harabasz scores indicate a more dispersed embedding structure. Δ denotes *After* minus *Before*.

Silhouette			Calinski–Harabasz		
Before	After	Δ	Before	After	Δ
0.132	0.091	-0.041	83.231	65.624	-18.393

Table 7: Community 3 and its top-5 popular movies.

Community 3	
Movie Name	Genres
<i>The Net</i>	Sci-Fi, Thriller
<i>Hoodlum</i>	Crime, Film-Noir
<i>Hellraiser</i>	Horror, Sci-Fi
<i>Aladdin and the King of Thieves</i>	Children’s
<i>Bound</i>	Crime, Thriller

Table 6 and Figure 6 illustrate the embedding structure before and after ICPNS fine-tuning. After applying ICPNS, the embedding space becomes more dispersed, with reduced cluster compactness, indicating that the model shifts from coarse community-level grouping toward more fine-grained and personalized user representations.

As shown in Table 7, *Aladdin and the King of Thieves*, a children-oriented movie, appears in Community 3 alongside predominantly adult-oriented films such as *Hellraiser* and *Hoodlum*. Despite its high popularity, *Aladdin and the King of Thieves* is unlikely to match the preferences of users favoring adult-oriented content within this community and therefore constitutes an informative negative candidate. By accounting for in-community popularity, ICPNS is able to identify such preference-misaligned popular items as effective negative samples.

5 Related Work

Learning from implicit feedback is challenging due to the absence of explicit negative signals. To address this issue, existing negative

sampling strategies can be broadly categorized into three groups: RNS, PNS and HNS. Below, we briefly review these strategies and representative recommender systems that adopt them.

Random Negative Sampling. RNS uniformly samples negative instances from items with no observed user interactions[7, 8, 12, 22, 26, 28]. Owing to its simplicity and low computational overhead, RNS has been widely adopted in collaborative filtering and graph-based recommendation models, especially in large-scale settings. Random sampling also introduces stochasticity, which can enhance item exploration and alleviate overfitting. However, RNS does not guarantee the quality or informativeness of sampled negatives, as many randomly selected items may be trivially irrelevant to the user. Several studies such as TDM[34] attempt to improve uniform random sampling under structured settings, such as hierarchical item trees or sequential recommendation.

Popularity Negative Sampling. PNS selects negative samples based on the popularity of items, that is, the more popular the item is, the more likely it is to be selected as the negative samples. Relying on the assumption that the popularity of items may demonstrate users’ global preferences, a series of popularity-based methods such as WBPR[6], HRNN[20] and BINN[15] typically assign sampling weights to items based on their frequency. This encourages the recommender to incorporate more popular items as negative samples into the training process. For quick updating the recommender parameters with the new incoming data, eALS[10] assigns the weight of missing data based on the popularity of items by an incremental update strategy. SoftRec[5] allows some unobserved items to have non-zero supervisory signals by generating soft targets with popularity distribution, thereby incorporating more unobserved knowledge into the training process.

Hard Negative Sampling. HNS takes another philosophy, it hypothesizes that any unobserved item should not be ranked higher than any observed positive item and subsequently oversamples items top-ranked by the recommender from the randomly selected candidates. To be more specific, HNS generally selects the item from the randomly selected item candidates who has the highest rating given by current system[11, 13, 14, 18, 30, 31]. Notably, PinSage[30] argues that the highest-scored item is likely to be a potentially positive sample, leading to the false negative problem.

6 Conclusion

In this work, we revisit negative sampling from the perspective of reliability and formalize three essential criteria (realness, hardness, and interpretability) that a negative sampling strategy should satisfy. Motivated by the observation that item exposure is structured by latent user communities, we propose ICPNS, a simple yet effective framework that leverages in-community popularity signals to identify reliable negative samples. Extensive experiments show that ICPNS yields consistent gains on graph-based models and competitive performance on MF-based models. By explicitly connecting negative sampling with exposure modeling at the community level, this work offers a new and interpretable direction for designing reliable negative sampling strategies in recommender systems.

References

- [1] Xuheng Cai, Chao Huang, Lianghao Xia, and Xubin Ren. 2023. LightGCL: Simple Yet Effective Graph Contrastive Learning for Recommendation. In *The Eleventh*

- International Conference on Learning Representations.*
- [2] Jiawei Chen, Can Wang, Sheng Zhou, Qihao Shi, Jingbang Chen, Yan Feng, and Chun Chen. 2020. Fast Adaptively Weighted Matrix Factorization for Recommendation with Implicit Feedback. arXiv:2003.01892 [cs.IR] <https://arxiv.org/abs/2003.01892>
 - [3] Ligu Chen, Zhigang Gong, Hong Xie, and Mingqiang Zhou. 2024. *False Negative Sample Aware Negative Sampling for Recommendation*. 195–206. doi:10.1007/978-981-97-2262-4_16
 - [4] Mingyue Cheng, Fajie Yuan, Qi Liu, Shenyang Ge, Zhi Li, Runlong Yu, Defu Lian, Senchao Yuan, and Enhong Chen. 2021. Learning Recommender Systems with Implicit Feedback via Soft Target Enhancement. In *Proceedings of the 44th International ACM SIGIR Conference on Research and Development in Information Retrieval* (Virtual Event, Canada) (SIGIR '21). Association for Computing Machinery, New York, NY, USA, 575–584. doi:10.1145/3404835.3462863
 - [5] Mingyue Cheng, Fajie Yuan, Qi Liu, Shenyang Ge, Zhi Li, Runlong Yu, Defu Lian, Senchao Yuan, and Enhong Chen. 2021. Learning Recommender Systems with Implicit Feedback via Soft Target Enhancement. In *Proceedings of the 44th International ACM SIGIR Conference on Research and Development in Information Retrieval* (Virtual Event, Canada) (SIGIR '21). Association for Computing Machinery, New York, NY, USA, 575–584. doi:10.1145/3404835.3462863
 - [6] Zeno Gantner, Lucas Drumond, Christoph Freudenthaler, and Lars Schmidt-Thieme. 2012. Personalized Ranking for Non-Uniformly Sampled Items. In *Proceedings of KDD Cup 2011 (Proceedings of Machine Learning Research, Vol. 18)*, Gideon Dror, Yehuda Koren, and Markus Weimer (Eds.). PMLR, 231–247. <https://proceedings.mlr.press/v18/gantner12a.html>
 - [7] Xiangnan He, Kuan Deng, Xiang Wang, Yan Li, YongDong Zhang, and Meng Wang. 2020. LightGCN: Simplifying and Powering Graph Convolution Network for Recommendation. In *Proceedings of the 43rd International ACM SIGIR Conference on Research and Development in Information Retrieval* (Virtual Event, China) (SIGIR '20). Association for Computing Machinery, New York, NY, USA, 639–648. doi:10.1145/3397271.3401063
 - [8] Xiangnan He, Lizi Liao, Hanwang Zhang, Liqiang Nie, Xia Hu, and Tat-Seng Chua. 2017. Neural Collaborative Filtering. In *Proceedings of the 26th International Conference on World Wide Web* (Perth, Australia) (WWW '17). International World Wide Web Conferences Steering Committee, Republic and Canton of Geneva, CHE, 173–182. doi:10.1145/3038912.3052569
 - [9] Xiangnan He, Hanwang Zhang, Min-Yen Kan, and Tat-Seng Chua. 2016. Fast Matrix Factorization for Online Recommendation with Implicit Feedback. In *Proceedings of the 39th International ACM SIGIR Conference on Research and Development in Information Retrieval* (Pisa, Italy) (SIGIR '16). Association for Computing Machinery, New York, NY, USA, 549–558. doi:10.1145/2911451.2911489
 - [10] Xiangnan He, Hanwang Zhang, Min-Yen Kan, and Tat-Seng Chua. 2017. Fast Matrix Factorization for Online Recommendation with Implicit Feedback. arXiv:1708.05024 [cs.IR] <https://arxiv.org/abs/1708.05024>
 - [11] Binbin Hu, Chuan Shi, Wayne Xin Zhao, and Philip S. Yu. 2018. Leveraging Meta-path based Context for Top-N Recommendation with A Neural Co-Attention Model. In *Proceedings of the 24th ACM SIGKDD International Conference on Knowledge Discovery & Data Mining* (London, United Kingdom) (KDD '18). Association for Computing Machinery, New York, NY, USA, 1531–1540. doi:10.1145/3219819.3219965
 - [12] Yiheng Jiang, Yongjian Yang, Yuanbo Xu, and En Wang. 2024. Spatial-Temporal Interval Aware Individual Future Trajectory Prediction. *IEEE Transactions on Knowledge and Data Engineering* 36, 10 (2024), 5374–5387. doi:10.1109/TKDE.2023.3332929
 - [13] Riwei Lai, Rui Chen, Qilong Han, Chi Zhang, and Li Chen. 2024. Adaptive Hardness Negative Sampling for Collaborative Filtering. *Proceedings of the AAAI Conference on Artificial Intelligence* 38, 8 (Mar. 2024), 8645–8652. doi:10.1609/aaai.v38i8.28709
 - [14] Yang Li, Yadan Luo, and Zi Huang. 2020. Fashion Recommendation with Multi-relational Representation Learning. In *Advances in Knowledge Discovery and Data Mining: 24th Pacific-Asia Conference, PAKDD 2020, Singapore, May 11–14, 2020, Proceedings, Part I* (Singapore, Singapore). Springer-Verlag, Berlin, Heidelberg, 3–15. doi:10.1007/978-3-030-47426-3_1
 - [15] Zhi Li, Hongke Zhao, Qi Liu, Zhenya Huang, Tao Mei, and Enhong Chen. 2018. Learning from History and Present: Next-item Recommendation via Discriminatively Exploiting User Behaviors. In *Proceedings of the 24th ACM SIGKDD International Conference on Knowledge Discovery & Data Mining* (London, United Kingdom) (KDD '18). Association for Computing Machinery, New York, NY, USA, 1734–1743. doi:10.1145/3219819.3220014
 - [16] Dawen Liang, Laurent Charlin, James McInerney, and David M. Blei. 2016. Modeling User Exposure in Recommendation. In *Proceedings of the 25th International Conference on World Wide Web* (Montréal, Québec, Canada) (WWW '16). International World Wide Web Conferences Steering Committee, Republic and Canton of Geneva, CHE, 951–961. doi:10.1145/2872427.2883090
 - [17] Haokai Ma, Ruobing Xie, Lei Meng, Xin Chen, Xu Zhang, Leyu Lin, and Jie Zhou. 2023. Exploring False Hard Negative Sample in Cross-Domain Recommendation. In *Proceedings of the 17th ACM Conference on Recommender Systems* (Singapore, Singapore) (RecSys '23). Association for Computing Machinery, New York, NY, USA, 502–514. doi:10.1145/3604915.3608791
 - [18] Haokai Ma, Ruobing Xie, Lei Meng, Fuli Feng, Xiaoyu Du, Xingwu Sun, Zhanhui Kang, and Xiangxu Meng. 2025. Negative Sampling in Recommendation: A Survey and Future Directions. arXiv:2409.07237 [cs.IR] <https://arxiv.org/abs/2409.07237>
 - [19] Gergely Palla, Imre Derényi, Illés Farkas, and Tamás Vicsek. 2005. Uncovering the overlapping community structure of complex networks in nature and society. *Nature* 435 (07 2005), 814–818.
 - [20] Massimo Quadrana, Alexandros Karatzoglou, Balázs Hidasi, and Paolo Cremonesi. 2017. Personalizing Session-based Recommendations with Hierarchical Recurrent Neural Networks. In *Proceedings of the Eleventh ACM Conference on Recommender Systems* (Como, Italy) (RecSys '17). Association for Computing Machinery, New York, NY, USA, 130–137. doi:10.1145/3109859.3109896
 - [21] Steffen Rendle and Christoph Freudenthaler. 2014. Improving pairwise learning for item recommendation from implicit feedback. In *Proceedings of the 7th ACM International Conference on Web Search and Data Mining* (New York, New York, USA) (WSDM '14). Association for Computing Machinery, New York, NY, USA, 273–282. doi:10.1145/2556195.2556248
 - [22] Steffen Rendle, Christoph Freudenthaler, Zeno Gantner, and Lars Schmidt-Thieme. 2009. BPR: Bayesian Personalized Ranking from Implicit Feedback. In *UAI 2009, Proceedings of the Twenty-Fifth Conference on Uncertainty in Artificial Intelligence, Montreal, QC, Canada, June 18–21, 2009*, Jeff A. Bilmes and Andrew Y. Ng (Eds.). AUAI Press, 452–461.
 - [23] Kexin Shi, Yun Zhang, Bingyi Jing, and Wenjia Wang. 2024. Enhancing Recommender Systems: A Strategy to Mitigate False Negative Impact. arXiv:2211.13912 [cs.IR] <https://arxiv.org/abs/2211.13912>
 - [24] Wentao Shi, Jiawei Chen, Fuli Feng, Jizhi Zhang, Junkang Wu, Chongming Gao, and Xiangnan He. 2023. On the Theories Behind Hard Negative Sampling for Recommendation. In *Proceedings of the ACM Web Conference 2023* (WWW '23). ACM, 812–822. doi:10.1145/3543507.3583223
 - [25] Xiang Wang, Xiangnan He, Meng Wang, Fuli Feng, and Tat-Seng Chua. 2019. Neural Graph Collaborative Filtering. In *Proceedings of the 42nd International ACM SIGIR* (Paris, France) (SIGIR '19). Association for Computing Machinery, New York, NY, USA, 165–174. doi:10.1145/3331184.3331267
 - [26] Yuanbo Xu, En Wang, Yongjian Yang, and Yi Chang. 2022. A Unified Collaborative Representation Learning for Neural-Network Based Recommender Systems. *IEEE Transactions on Knowledge and Data Engineering* 34, 11 (2022), 5126–5139. doi:10.1109/TKDE.2021.3054782
 - [27] Hong-Jian Xue, Xin-Yu Dai, Jianbing Zhang, Shujian Huang, and Jiajun Chen. 2017. Deep matrix factorization models for recommender systems. In *Proceedings of the 26th International Joint Conference on Artificial Intelligence* (Melbourne, Australia) (IJCAI '17). AAAI Press, 3203–3209.
 - [28] Yuhao Yang, Chao Huang, Lianhao Xia, Yuxuan Liang, Yanwei Yu, and Chenliang Li. 2022. Multi-Behavior Hypergraph-Enhanced Transformer for Sequential Recommendation. In *Proceedings of the 28th ACM SIGKDD Conference on Knowledge Discovery and Data Mining* (Washington DC, USA) (KDD '22). Association for Computing Machinery, New York, NY, USA, 2263–2274. doi:10.1145/3534678.3539342
 - [29] Zhen Yang, Ming Ding, Chang Zhou, Hongxia Yang, Jingren Zhou, and Jie Tang. 2020. Understanding Negative Sampling in Graph Representation Learning. In *Proceedings of the 26th ACM SIGKDD International Conference on Knowledge Discovery & Data Mining* (Virtual Event, CA, USA) (KDD '20). Association for Computing Machinery, New York, NY, USA, 1666–1676. doi:10.1145/3394486.3403218
 - [30] Rex Ying, Ruining He, Kaifeng Chen, Pong Eksombatchai, William L. Hamilton, and Jure Leskovec. 2018. Graph Convolutional Neural Networks for Web-Scale Recommender Systems. In *Proceedings of the 24th ACM SIGKDD International Conference on Knowledge Discovery & Data Mining* (London, United Kingdom) (KDD '18). Association for Computing Machinery, New York, NY, USA, 974–983. doi:10.1145/3219819.3219890
 - [31] Weinan Zhang, Tianqi Chen, Jun Wang, and Yong Yu. 2013. Optimizing top-n collaborative filtering via dynamic negative item sampling. In *Proceedings of the 36th International ACM SIGIR Conference on Research and Development in Information Retrieval* (Dublin, Ireland) (SIGIR '13). Association for Computing Machinery, New York, NY, USA, 785–788. doi:10.1145/2484028.2484126
 - [32] Wayne Xin Zhao, Shanlei Mu, Yupeng Hou, Zihan Lin, Yushuo Chen, Xingyu Pan, Kaiyuan Li, Yujie Lu, Hui Wang, Changxin Tian, Yingqian Min, Zhichao Feng, Xinyan Fan, Xu Chen, Pengfei Wang, Wendi Ji, Yaliang Li, Xiaoling Wang, and Ji-Rong Wen. 2021. RecBole: Towards a Unified, Comprehensive and Efficient Framework for Recommendation Algorithms. In *CIKM*. ACM, 4653–4664.
 - [33] Tao Zhou. 2011. Understanding Online Community User Participation: A Social Influence Perspective. *Internet Res.* 21 (2011), 67–81. <https://api.semanticscholar.org/CorpusID:15351993>
 - [34] Han Zhu, Xiang Li, Pengye Zhang, Guozheng Li, Jie He, Han Li, and Kun Gai. 2018. Learning Tree-based Deep Model for Recommender Systems. In *Proceedings of the 24th ACM SIGKDD International Conference on Knowledge Discovery & Data Mining* (London, United Kingdom) (KDD '18). Association for Computing Machinery, New York, NY, USA, 1079–1088. doi:10.1145/3219819.3219826

A Two Stage Training Pipeline

Algorithm 1: Two-Stage Training Pipeline with ICPNS

Input: Interaction matrix X , number of communities P , smoothing factor α , learning rate η
Output: Optimized model parameters Θ^*

- 1 Initialize model parameters Θ ;
- 2 **while** *not converged* **do**
- 3 Sample a mini-batch of positive interactions
 $\mathcal{B} = \{(u, i) \mid x_{ui} = 1\}$;
- 4 For each $(u, i) \in \mathcal{B}$, sample $i^- \sim \text{Uniform}(\mathcal{I} \setminus \mathcal{I}_u^+)$;
- 5 Update Θ by minimizing the BPR loss;
- 6 **end**
- 7 Extract user embeddings $E_U \leftarrow \text{Encoder}(X; \Theta)$;
- 8 Cluster users into P disjoint communities $\{C_1, \dots, C_P\}$ using E_U ;
- 9 **for** $p = 1$ **to** P **do**
- 10 Compute in-community interaction counts ν_p via Eq. (10);
- 11 Compute smoothed popularity s_p via Eq. (11);
- 12 Construct alias table \mathcal{T}_p from s_p ;
- 13 **end**
- 14 **while** *not converged* **do**
- 15 Sample a mini-batch of positive interactions
 $\mathcal{B} = \{(u, i) \mid x_{ui} = 1\}$;
- 16 **foreach** $(u, i) \in \mathcal{B}$ **do**
- 17 Identify community C_p such that $u \in C_p$;
- 18 Sample $i^- \sim \text{Alias}(\mathcal{T}_p)$ **subject to** $i^- \in \mathcal{I} \setminus \mathcal{I}_u^+$;
- 19 **end**
- 20 Update Θ by minimizing the BPR loss;
- 21 **end**
- 22 **return** Θ^*

B Additional Experiment

B.1 Realness of Samples

In implicit feedback recommendation, negative samples are not directly observable, which makes it challenging to assess their reliability. Beyond evaluating negative sampling strategies through ranking performance, we introduce an auxiliary diagnostic metric to examine whether sampled negatives correspond to withheld positive interactions.

We define **HoldoutHit** to quantify the probability that a sampled negative item appears in the holdout positive set. For each user, we record the items sampled as negatives during training and check whether these items occur among the user’s validation interactions. Since the validation set consists of positive interactions withheld from training, an overlap indicates that the sampled negative item is a potential false negative with respect to future interactions.

Formally, let $\mathcal{N}_u^{(K)}$ denote the set of K negative items sampled for user u during training, and let $\mathcal{S}_u^{\text{val}}$ denote the set of validation positives for the same user. The HoldoutHit metric is defined as

$$\text{HoldoutHit}@K = \mathbb{E}_u \left[\frac{|\mathcal{N}_u^{(K)} \cap \mathcal{S}_u^{\text{val}}|}{K} \right]. \quad (13)$$

The HoldoutHit@10 results are reported in Figure [?]. HNS attains the highest value, indicating a higher likelihood of sampling

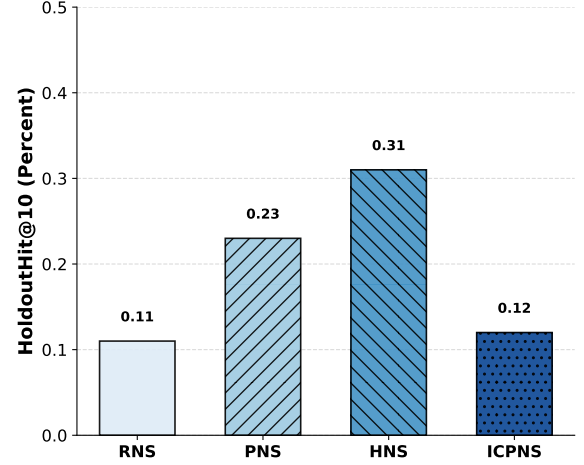


Figure 7: on ML-100K

items that later appear as validation positives. PNS also exhibits an elevated HoldoutHit, reflecting the tendency of popular items to reoccur in future interactions. In contrast, ICPNS yields a lower HoldoutHit than both HNS and PNS, while remaining higher than random sampling.

Random negative sampling (RNS) achieves the lowest HoldoutHit score. This behavior can be attributed to its uniform sampling strategy and the high sparsity of the dataset, under which randomly sampled items are unlikely to coincide with withheld positives. However, a low HoldoutHit does not necessarily imply higher negative-sample realness, as it may also result from sampling items that are irrelevant or unexposed to the user.

Overall, HoldoutHit captures the risk of sampling potential false negatives with respect to future interactions, but it is not equivalent to the exposure-based notion of realness considered in this work and should be interpreted as a complementary diagnostic metric.

B.2 Hyperparameter Analysis

Number of Communities P . As illustrated in Figure 8(a) and (b), performance on both datasets improves as P increases from small to moderate values and then saturates or slightly declines. On ML-1M, both NDCG and Recall consistently increase with larger P , indicating that finer-grained community structures are effective when sufficient interaction data are available. On Yelp, performance peaks at $P = 32$ and exhibits a mild degradation at $P = 64$, suggesting diminishing returns from overly fine partitioning. Overall, moderate-to-large values of P provide stable and competitive performance on large-scale datasets.

Popularity Smoothing Factor α . Figure 8 (c) and (d) show that both ML-1M and Yelp favor relatively small smoothing factors. The best performance is achieved when $\alpha \in [0.1, 0.4]$, while increasing α to 0.8 leads to a consistent performance drop. This trend indicates that excessive smoothing weakens the discriminative power of in-community popularity signals on large-scale data.

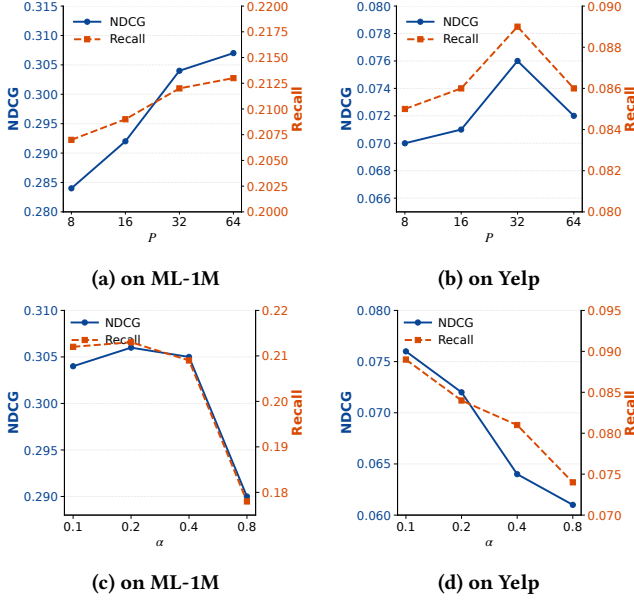


Figure 8: Parameter sensitivity analysis of ICPNS on ML-1M and Yelp. The top row (a–b) illustrates the impact of P , while the bottom row (c–d) displays the effect of α .

B.3 Fair warm-up protocol

In some cases, a model may benefit from continued optimization even after apparent convergence during pretraining. To ensure a fair and controlled comparison between different negative sampling strategies, we adopt a unified warm-up protocol for all methods.

Specifically, we first pretrain the model using a common baseline sampler until convergence. Starting from the same pretrained checkpoint, we then perform a second-stage fine-tuning procedure, during which only the negative sampling strategy is changed while all other training configurations remain identical. This two-stage pipeline isolates the effect of negative sampling from initialization and optimization factors.

Under this protocol, we compare RNS and ICPNS using LightGCN as a fixed backbone by measuring the relative improvement in NDCG@10 on the ML-100K dataset during the fine-tuning stage. As illustrated in Figure 9, both methods start from the same performance level at the beginning of fine-tuning, ensuring that any subsequent performance divergence can be attributed solely to the difference in negative sampling strategies rather than discrepancies in model warm-up or convergence behavior.

C Metrics

C.1 Recommendation Metrics

In this work, we evaluate recommendation performance using standard top- K ranking metrics, including Recall@ K , NDCG@ K , MRR@ K , and Precision@ K . These metrics characterize complementary aspects of recommendation quality, such as coverage of relevant items, ranking sensitivity, early-hit behavior, and recommendation accuracy.

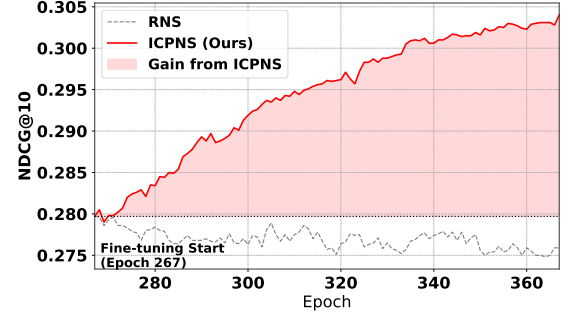


Figure 9: NDCG@10 trajectories during fine-tuning on ML-100K. Both methods start from the same pretrained checkpoint at Epoch 267. ICPNS consistently improves performance over RNS under the same warm-up protocol.

Let U denote the set of users. For a user $u \in U$, let $R(u)$ be the set of ground-truth relevant items, and $\hat{R}(u)$ be the ranked recommendation list truncated at K . We denote $|\cdot|$ as set cardinality.

C.1.1 Recall@ K . Recall@ K measures the fraction of relevant items that are successfully retrieved within the top- K recommendation list. It is defined as

$$\text{Recall@}K = \frac{1}{|U|} \sum_{u \in U} \frac{|\hat{R}(u) \cap R(u)|}{|R(u)|}. \quad (14)$$

Recall focuses on coverage of relevant items and does not consider their exact ranking positions.

C.1.2 NDCG@ K . Normalized Discounted Cumulative Gain (NDCG) evaluates ranking quality by accounting for the positions of relevant items, assigning higher importance to items ranked near the top. NDCG@ K is defined as

$$\text{NDCG@}K = \frac{1}{|U|} \sum_{u \in U} \left(\frac{\sum_{i=1}^K \mathbb{1}(i \in R(u)) \cdot \frac{1}{\log_2(i+1)}}{\sum_{i=1}^{\min(|R(u)|, K)} \frac{1}{\log_2(i+1)}} \right), \quad (15)$$

where $\mathbb{1}(\cdot)$ is the indicator function. The denominator corresponds to the ideal DCG obtained by ranking all relevant items at the top positions.

C.1.3 MRR@ K . Mean Reciprocal Rank (MRR) measures how early the first relevant item appears in the ranked list. It is defined as

$$\text{MRR@}K = \frac{1}{|U|} \sum_{u \in U} \frac{1}{\text{rank}_u^*}, \quad (16)$$

where rank_u^* denotes the rank position of the first relevant item for user u within the top- K list. If no relevant item appears in the top- K recommendations, the contribution for that user is set to zero. MRR emphasizes early-hit performance.

C.1.4 Precision@ K . Precision@ K measures the fraction of recommended items that are relevant. It evaluates the accuracy of the top- K recommendation list and is defined as

$$\text{Precision@}K = \frac{1}{|U|} \sum_{u \in U} \frac{|\hat{R}(u) \cap R(u)|}{|\hat{R}(u)|}. \quad (17)$$

Precision@K focuses on the purity of the recommendation list and complements Recall@K by reflecting how many recommended items are relevant.

C.2 Clustering Metrics

To evaluate the quality of user community structures, we additionally adopt two widely used internal clustering validation metrics: the Silhouette score and the Calinski–Harabasz index. Both metrics assess clustering compactness and separation without requiring external labels.

C.2.1 Silhouette. The Silhouette score measures how well each sample fits within its assigned cluster compared to other clusters. For a data point i , let $a(i)$ denote the average distance between i and all other points in the same cluster, and let $b(i)$ denote the minimum average distance between i and points in any other cluster. The Silhouette coefficient for i is defined as

$$s(i) = \frac{b(i) - a(i)}{\max\{a(i), b(i)\}}. \quad (18)$$

The overall Silhouette score is obtained by averaging $s(i)$ over all samples.

C.2.2 Calinski–Harabasz Index. The Calinski–Harabasz (CH) index evaluates clustering quality by comparing between-cluster dispersion with within-cluster dispersion. It is defined as

$$\text{CH} = \frac{\text{Tr}(B_k)}{\text{Tr}(W_k)} \cdot \frac{n - k}{k - 1}, \quad (19)$$

where n is the total number of samples, k is the number of clusters, $\text{Tr}(B_k)$ denotes the trace of the between-cluster dispersion matrix, and $\text{Tr}(W_k)$ denotes the trace of the within-cluster dispersion matrix.